$2\beta_s$ *Measurement at LHCb*

Géraldine Conti and the LHCb Collaboration

ÉCOLE POLYTECHNIQUE FÉDÉRALE DE LAUSANNE

geraldine.conti@epfl.ch

Abstract

A measurement of $2\beta_s$, the phase of the $\mathrm{B_s^0}$–$\mathrm{\overline{B}_s^0}$ oscillation amplitude with respect to that of the $\mathrm{b \to c^+W^-}$ tree decay amplitude, is one of the key goals of the LHCb experiment with first data. In the Standard Model (SM), $2\beta_s$ is predicted to be $0.0360^{+0.0020}_{-0.0016}\,\mathrm{rad}$. The current constraints from the Tevatron are: $2\beta_s \in [0.32; 2.82]$ at 68%CL from the CDF experiment and $2\beta_s = 0.57^{+0.24}_{-0.30}$ from the DØ experiment. Although the statistical uncertainties are large, these results hint at the possible contribution of New Physics in the $\mathrm{B_s^0}$–$\mathrm{\overline{B}_s^0}$ box diagram. After one year of data taking at LHCb at an average luminosity of $\mathcal{L} \sim 2 \cdot 10^{32}\,\mathrm{cm^{-2}\,s^{-1}}$ (integrated luminosity $\mathcal{L}_{\mathrm{int}} \sim 2\,\mathrm{fb^{-1}}$), the expected statistical uncertainty on the measurement is $\sigma(2\beta_s) \simeq 0.03$. This uncertainty is similar to the $2\beta_s$ value predicted by the SM.

Phenomenology

$\mathrm{B_s^0}$ mesons can **decay into** $J/\psi\phi$ through tree and penguin processes (Fig. 1), but the tree diagram dominates, which has a single weak phase :

$$\Phi_{\mathrm{D}} = \arg(V_{cs}V_{cb}^*).$$

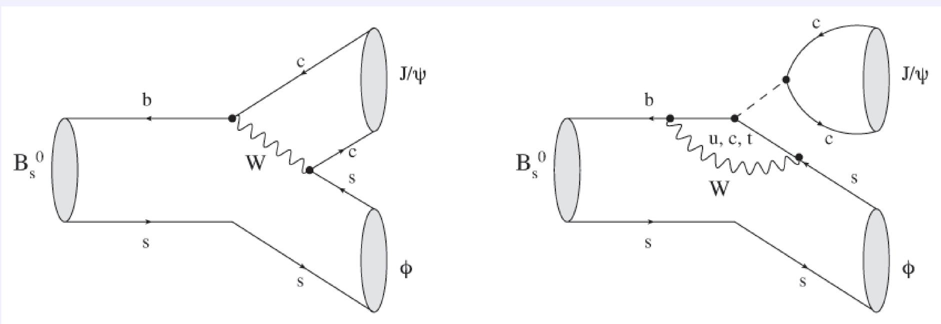

Fig. 1. Decay topologies contributing to $\mathrm{B_s^0} \to J/\psi\phi$ within the SM.

Before decaying into $J/\psi\phi$, $\mathrm{B_s^0}$ mesons can also **first oscillate into** $\mathrm{\overline{B}_s^0}$, with a $\mathrm{B_s^0}$ mixing phase :

$$\Phi_{\mathrm{M}} = 2\arg(V_{ts}V_{tb}^*).$$

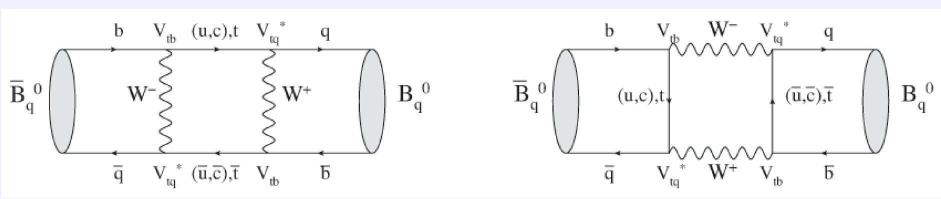

Fig. 2. Diagrams responsible of $\mathrm{B_q}$–$\mathrm{\overline{B}_q}$ mixing, within the Standard Model (q=s,d).

The **interference** between the two possible paths to $J/\psi\phi$ gives rise to the CP violating phase :

$$\Phi_{J/\psi\phi} = \Phi_{\mathrm{M}} - 2\Phi_{\mathrm{D}} = -2 \cdot \underbrace{\arg(-V_{ts}V_{tb}^*/V_{cs}V_{cb}^*)}_{\beta_s}.$$

New physics could appear as new particles contributing to the box diagrams in Fig. 2.

$\mathrm{B_s^0} \to J/\psi\phi$ is a pseudo-scalar to vector-vector decay. The final state is an **admixture of CP-even** (ℓ=0,2) **and CP-odd** (ℓ=1) **states**, ℓ being the orbital momentum between J/ψ and ϕ. An **angular analysis** of the decay products is required to disentangle statistically the components. The decay product angles $\Omega = \{\theta, \varphi, \psi\}$ are given in Fig. 3.

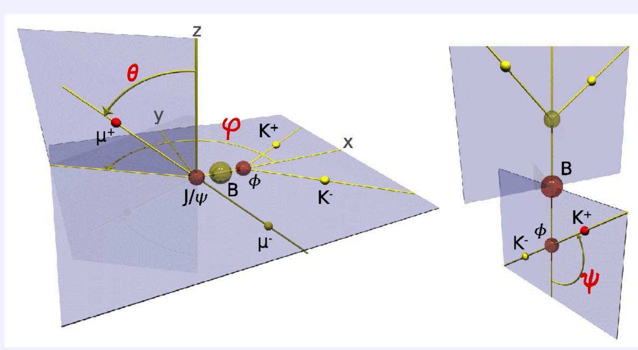

Fig. 3. Decay product angles $\Omega = \{\theta, \varphi, \psi\}$ in the transversity basis.

Analysis

$2\beta_s$ is obtained from the fit of the theoretical expressions of differential decay rates. We need to:

- trigger and select $\mathrm{B_s^0} \to J/\psi\phi$ events ;
- measure their propertime ;
- measure the transversity angles of their decay products ;
- tag their initial flavour.

$\mathrm{B^0} \to J/\psi\mathrm{K^{*0}}$ and $\mathrm{B^+} \to J/\psi\mathrm{K^+}$ are used as **control channels** in different parts of the analysis.

Triggering and Selection

Ideally, the $\mathrm{B_s^0} \to J/\psi\phi$ selection is :

- **Efficient** : to select the highest signal yield possible with a reasonable background level.
- **Unbiased** : to minimize the lifetime and angular acceptance distortions (Fig. 4).

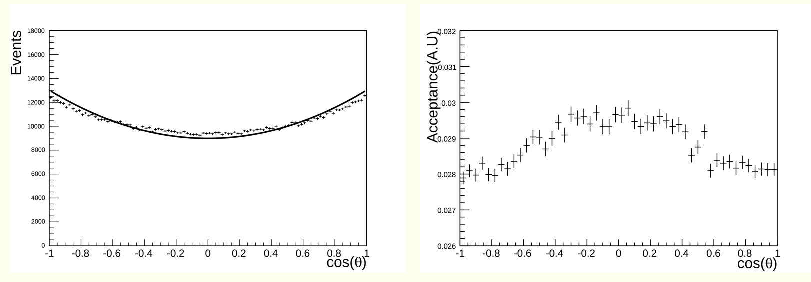

Fig. 4. $\cos(\theta)$ distribution (left, theory superposed) and acceptance (right).

- **As common as possible for the signal and control channels** : to ensure the same phase space (Fig. 5).

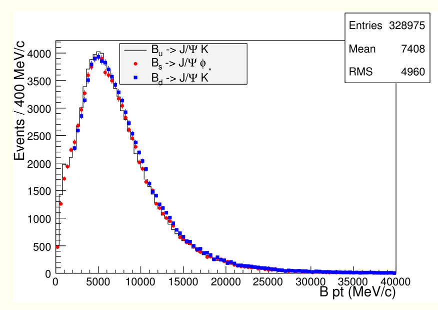

Fig. 5. p_T distributions for $\mathrm{B_s^0}$, $\mathrm{B^0}$ and $\mathrm{B^+}$ candidates after selection.

The **trigger (Level-0 (L0) + HLT)** should fulfill the requirements above. The selection efficiency ϵ_{tot} and the event yield for triggered events are given in Tab. 1.

Channel	ϵ_{tot} [%]	Event yield after L0	Event yield after L0+HLT
$\mathrm{B_s^0} \to J/\psi(\mu\mu)\phi(\mathrm{KK})$	2.61 ± 0.01	156 k	117 k
$\mathrm{B^0} \to J/\psi(\mu\mu)\mathrm{K^{*0}}(\mathrm{K}\pi)$	1.54 ± 0.01	648 k	489 k
$\mathrm{B^+} \to J/\psi(\mu\mu)\mathrm{K^+}$	2.61 ± 0.01	1 248 k	942 k

Tab. 1. Total selection efficiency ϵ_{tot} (no HLT) and and untagged event yield for selected and L0/L0+HLT triggered events.

Backgrounds

Prompt background ($t < 0.2\,\mathrm{ps}$) (Fig. 6) :

- All tracks come from the primary vertex.

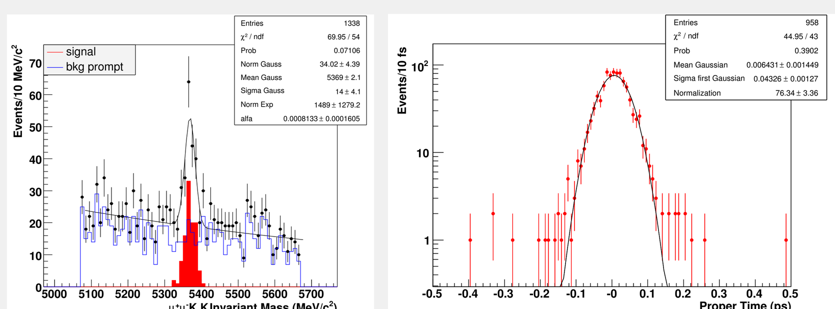

Fig. 6. Mass (left) and proper time distribution (right) for the prompt category.

Long-lived background (Fig. 7) :

- ≥ 1 of the tracks comes from the secondary vertices of other b or c decays.

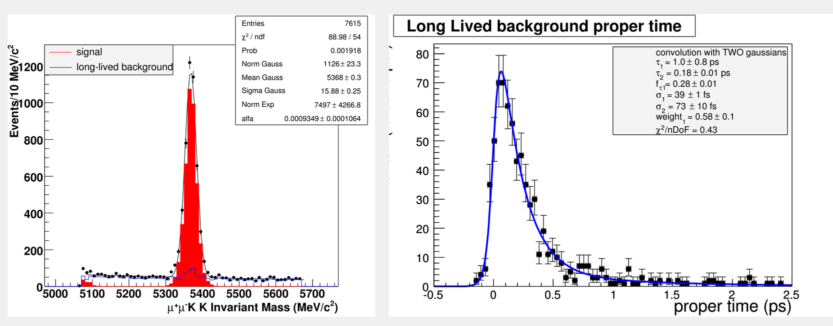

Fig. 7. Mass (left) and proper time distribution (right) for the long-lived category.

The B/S ratios are given in Tab. 2 :

Channel	B_{Pr}/S	B_{LL}/S	Minimum bias
$\mathrm{B_s^0} \to J/\psi(\mu\mu)\phi(\mathrm{KK})$	1.6 ± 0.6	0.51 ± 0.08	~ 0.3 Hz
$\mathrm{B^0} \to J/\psi(\mu\mu)\mathrm{K^{*0}}(\mathrm{K}\pi)$	5.2 ± 0.3	1.53 ± 0.08	~ 8.1 Hz
$\mathrm{B^+} \to J/\psi(\mu\mu)\mathrm{K^+}$	1.6 ± 0.2	0.29 ± 0.06	~ 1.4 Hz

Tab. 2. B/S ratios for prompt and long-lived categories ($\pm 50\,\mathrm{MeV}/c^2$ mass window) and minimum bias rate ($\pm 300\,\mathrm{MeV}/c^2$ mass window), after selection and L0.

Flavour Tagging

Flavour tagging is done by combining information of the **Opposite-Side** (OS) (μ, e, K, ...) and **Same-Side** (SS) (π, K) taggers. The effective efficiency $\varepsilon_{\mathrm{eff}}$, tagging efficiency $\varepsilon_{\mathrm{tag}}$ and mistag rate ω are given in Tab. 3.

Channel	$\varepsilon_{\mathrm{eff}}$	$\varepsilon_{\mathrm{tag}}$	ω
$\mathrm{B_s^0} \to J/\psi(\mu\mu)\phi(\mathrm{KK})$	6.23 ± 0.15	55.71 ± 0.17	33.27 ± 0.21
$\mathrm{B^0} \to J/\psi(\mu\mu)\mathrm{K^{*0}}(\mathrm{K}\pi)$	4.52 ± 0.11	53.60 ± 0.15	35.48 ± 0.19
$\mathrm{B^+} \to J/\psi(\mu\mu)\mathrm{K^+}$	4.45 ± 0.10	52.76 ± 0.14	35.48 ± 0.18

Tab. 3. Effective efficiency $\varepsilon_{\mathrm{eff}}$, tagging efficiency $\varepsilon_{\mathrm{tag}}$ and mistag rate ω.

Fitting

The likelihood function of N events is given by :

$$\mathcal{L} = \prod_e^N \mathcal{P}(X_e; \lambda)$$

Observables X_e = {t, Ω, m, flavour tag q}.
Physics Parameters $\lambda_{\mathbf{phys}}$ = $\{\Gamma_s, \Delta\Gamma_s, R_\perp, R_0, \delta_\perp, \delta_{||}, \Delta m_s, \beta_s\}$.
Detector Parameters $\lambda_{\mathbf{det}}$ = {resolutions $\sigma_{(m,t)}$, ω, background properties,... }.

PDF $\mathcal{P} = f_{\mathrm{sig}} \cdot S + f_{\mathrm{Pr}} \cdot B_{\mathrm{Pr}} + (1 - f_{\mathrm{sig}} - f_{\mathrm{Pr}}) \cdot B_{\mathrm{LL}}$

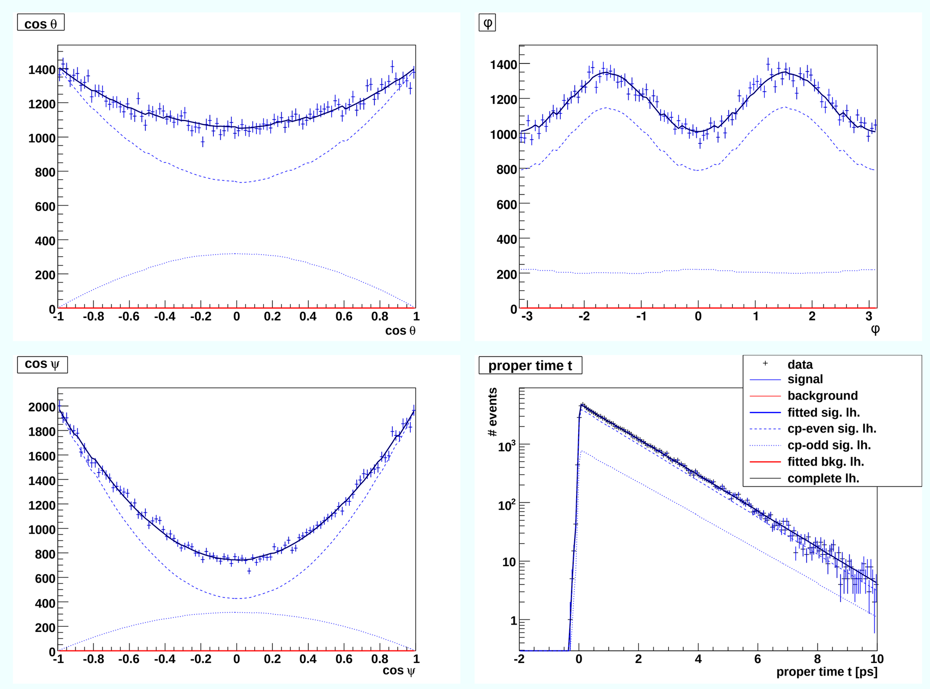

Fig. 8. Projections of data and fitted signal PDF on the angles and proper time, with CP-even (dashed) and CP-odd (dotted) components.

Sensitivity Study

A $2\beta_s$ **sensitivity study** has been performed with respect to the integrated luminosity $\mathcal{L}_{\mathrm{int}}$. At a value of $\mathcal{L}_{\mathrm{int}} \sim 2\,\mathrm{fb^{-1}}$ (one year of data taking at a 14TeV centre of mass energy), the statistical uncertainty on $2\beta_s$ will be $\sigma(2\beta_s) \simeq 0.03$ (Fig. 9).

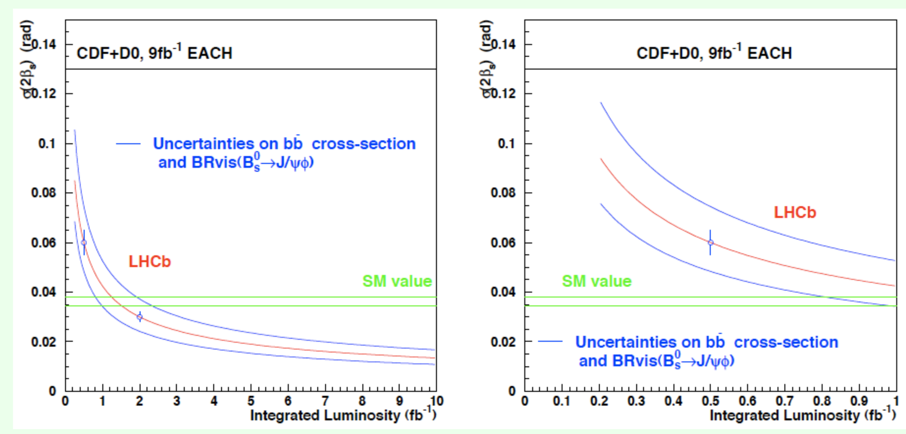

Fig. 9. Statistical uncertainty (red line) on $2\beta_s$ versus the integrated luminosity, bounded by the uncertainties coming from $\mathrm{b\bar{b}}$ cross-section and the visible BR on $\mathrm{B_s^0} \to J/\psi\phi$ (blue lines). The green band is the SM value.